RESEARCH ARTICLE

Hybrid Spreading Mechanisms and T Cell Activation Shape the Dynamics of HIV-1 Infection

Changwang Zhang[1,2,4], Shi Zhou[1], Elisabetta Groppelli[3], Pierre Pellegrino[5], Ian Williams[5], Persephone Borrow[6], Benjamin M. Chain[3‡]*, Clare Jolly[3‡]*

1 Department of Computer Science, University College London, London, United Kingdom, 2 Security Science Doctoral Research Training Centre, University College London, London, United Kingdom, 3 Division of Infection and Immunity, University College London, London, United Kingdom, 4 School of Computer Science, National University of Defense Technology, Changsha, China, 5 Centre for Sexual Health & HIV Research, Mortimer Market Centre, London, United Kingdom, 6 Nuffield Department of Medicine, University of Oxford, Oxford, United Kingdom

‡ These authors are joint last authors on this work.
* b.chain@ucl.ac.uk (BMC); c.jolly@ucl.ac.uk (CJ)

Abstract

HIV-1 can disseminate between susceptible cells by two mechanisms: cell-free infection following fluid-phase diffusion of virions and by highly-efficient direct cell-to-cell transmission at immune cell contacts. The contribution of this hybrid spreading mechanism, which is also a characteristic of some important computer worm outbreaks, to HIV-1 progression in vivo remains unknown. Here we present a new mathematical model that explicitly incorporates the ability of HIV-1 to use hybrid spreading mechanisms and evaluate the consequences for HIV-1 pathogenenesis. The model captures the major phases of the HIV-1 infection course of a cohort of treatment naive patients and also accurately predicts the results of the Short Pulse Anti-Retroviral Therapy at Seroconversion (SPARTAC) trial. Using this model we find that hybrid spreading is critical to seed and establish infection, and that cell-to-cell spread and increased CD4+ T cell activation are important for HIV-1 progression. Notably, the model predicts that cell-to-cell spread becomes increasingly effective as infection progresses and thus may present a considerable treatment barrier. Deriving predictions of various treatments' influence on HIV-1 progression highlights the importance of earlier intervention and suggests that treatments effectively targeting cell-to-cell HIV-1 spread can delay progression to AIDS. This study suggests that hybrid spreading is a fundamental feature of HIV infection, and provides the mathematical framework incorporating this feature with which to evaluate future therapeutic strategies.

Author Summary

The ability to spread using more than one mechanism, named hybrid spreading, is a ubiquitous feature of many real world epidemics including HIV and Hepatitis C virus infection

in vivo, and computer worms spreading on the Internet. Hybrid spreading of HIV is well documented experimentally but its importance to HIV progression has been unclear. In this paper, we introduce a mathematical model of HIV dynamics that explicitly incorporates hybrid spreading. The model output shows excellent agreement to two sets of clinical data from a treatment naive cohort and from the Short Pulse Anti-Retroviral Therapy at Seroconversion trial. The model demonstrates that hybrid spreading is an essential feature of HIV progression, a result which has significant implications for future therapeutic strategies against HIV.

Introduction

The course of HIV-1 infection is typified by three phases; acute infection characterized by a rapid viraemia peak (3–6 weeks post-infection) followed by a rapid fall in virus levels, a stable chronic phase of variable length characterized by low level viraemia and slowly declining $CD4^+$ T cell numbers, and a final stage (Acquired Immune Deficiency Syndrome, AIDS) characterized by multiple opportunistic infections and a rapid fall in $CD4^+$ T cell count. The cellular and viral changes which drive each phase of this complex infection have been the subject of intense debate, in which mathematical models have played an important role in delineating HIV-1 pathogenesis and informing antiretroviral therapy [1–3]. The rich literature appertaining to mathematical modeling of intra host HIV dynamics has been reviewed several times recently [1, 4–6]. Recent studies incorporate sophisticated models of immune selection [7, 8], as well as the formation of a latent reservoir of quiescent infected cells [9, 10]. However the interplay of cell-to-cell spread and increased $CD4^+$ T cell activation, that are likely to have profound influences on the progression of the disease have been hitherto little studied. Here we have addressed this and developed a unified model that can explain the complex progress of the infection in all its phases and its variable timescale. Such a unified model is important not only to understand the HIV-1 infection dynamics, but also to estimate the long term effects of therapeutic strategies on HIV-1 progression. In this paper, unless otherwise stated, "T cells" refers to $CD4^+$ T cells.

HIV-1 predominantly replicates in $CD4^+$ T cells *in vivo*, and is now known to spread between T cells by two parallel routes. According to the classical model of HIV-1 spread, virus particles bud from an infected T cell, enter the blood/extracellular fluid and then infect another T cell following a chance encounter (termed cell-free spread). Because diffusion of virus particles is much faster than cell migration, and there is extensive flow of blood and fluid, this mode of spreading can be characterized by a well mixed epidemic spreading model. In this scenario, the probability of infection for a particular cell will be proportional to the concentration of extracellular infectious virus. However, HIV-1 can also disseminate by direct transmission from one cell to another by a process of cell-to-cell spread. Two pathways of cell-to-cell transmission have been reported. Firstly, an infected T cell can transmit virus directly to a target T cell via a virological synapse [11–13]. Secondly, an antigen presenting cell (APC) can also transmit HIV-1 to T cells by a process that either involves productive infection (in the case of macrophages) or capture and transfer of virions *in trans* (in the case of dendritic cells) [11]. Whichever pathway is used, infection by cell-to-cell transfer is reported to be much more efficient than cell-free virus spread [14–16]. A number of factors contribute to this increased efficiency, including polarised virus budding towards the site of cell-to-cell contact, close apposition of cells which minimizes fluid-phase diffusion of virions, and clustering of HIV-1 entry receptors on the target cell to the contact zone [11, 12]. Cell-to-cell spread is thought to be particularly important

in lymphoid tissues where CD4$^+$ T lymphocytes are densely packed and likely to frequently interact. Indeed, intravital imaging studies have supported the concept of the HIV-1 virological synapse *in vivo* [17, 18].

Hybrid spreading is in fact a feature of other viral infections [19], but is also shared in other "epidemic" scenarios such as spread of computer worms [20, 21], or of mobile phone viruses [22]. The mathematical analysis of hybrid spreading has received significant previous attention [22–25]. However, the importance of hybrid spread to HIV-1 dissemination and disease progression, has not been explored from a mathematical point of view.

In this paper we develop a new mathematical model which incorporates the basic principles of previous host-centric models including a virus-dependent immune response [8], viral latency and a progressive increase in cell activation [26, 27]. Notably, the model additionally includes explicit terms for the two modes of virus spread, parametrised from experimental observation. The model faithfully replicates the overall three phase course of HIV-1 infection. The model predictions are consistent with both a set of longitudinal data (viral load and CD4$^+$ T cell count) from a cohort of treatment naive HIV-1 infected patients and the results of the Short Pulse Anti-Retroviral Therapy at Seroconversion (SPARTAC) trial that aims to evaluate how the short-course antiretroviral therapy (ART) delays HIV progression [28]. The results of our study reveal the importance of two modes of HIV-1 spread, highlight the close link between cell-to-cell spread and cell activation in driving the progression of HIV-1 infection to AIDS and support early therapeutic intervention (i.e. "test-and-treat" initiatives) to delay disease progression in infected individuals. Since cell-to-cell spread is likely to present a considerable barrier to HIV-1 eradication, our data suggest that efforts to target this mode of viral spread whilst simultaneously manipulating CD4$^+$ T cell activation may be a fruitful strategy to help control virus infection and halt progression to AIDS.

Results

The HIV-1 model

We here introduce a model of HIV-1 infection as depicted in Fig. 1A. We consider four distinct CD4$^+$ T cell states: activated, uninfected susceptible (*S*) cells; activated and productively infected (*I*) cells; quiescent, uninfected (*Q*) cells; and quiescent latently (*L*) infected cells. The total CD4$^+$ cell density (N) changes with time and is given by the sum of these four terms, i.e. $N(t) = Q(t) + S(t) + I(t) + L(t)$. The model can be described by an Ordinary Differential Equation (ODE) system (Equation 1) and is illustrated in Fig. 1A.

$$
\begin{aligned}
\frac{dQ}{dt} &= -\gamma Q + r_s S - a\frac{N_M}{N}Q + b \\
\frac{dS}{dt} &= -\gamma_s S - r_s S + a\frac{N_M}{N}Q - cI\frac{S}{N}\theta\beta_1 - SV\beta_2 + p\frac{N_M - N}{N_M}S \\
\frac{dI}{dt} &= -\gamma_I I - r_I I + a\frac{N_M}{N}L + cI\frac{S}{N}\theta\beta_1 + SV\beta_2 - \kappa\frac{I}{I+0.1}\frac{N}{N_M}I \\
\frac{dL}{dt} &= -\gamma L + r_I I - a\frac{N_M}{N}L \\
\frac{dV}{dt} &= -\gamma_V V + gI
\end{aligned}
\tag{1}
$$

The density variables (*Q, S, I, L, V*) and parameters are defined in Table 1. The densities are measured as numbers of cells or virions in a μl of blood/extracellular fluid. We set a density variable to zero when it drops to below $10^{-12}/\mu l$, accounting for the fact that when density of cells
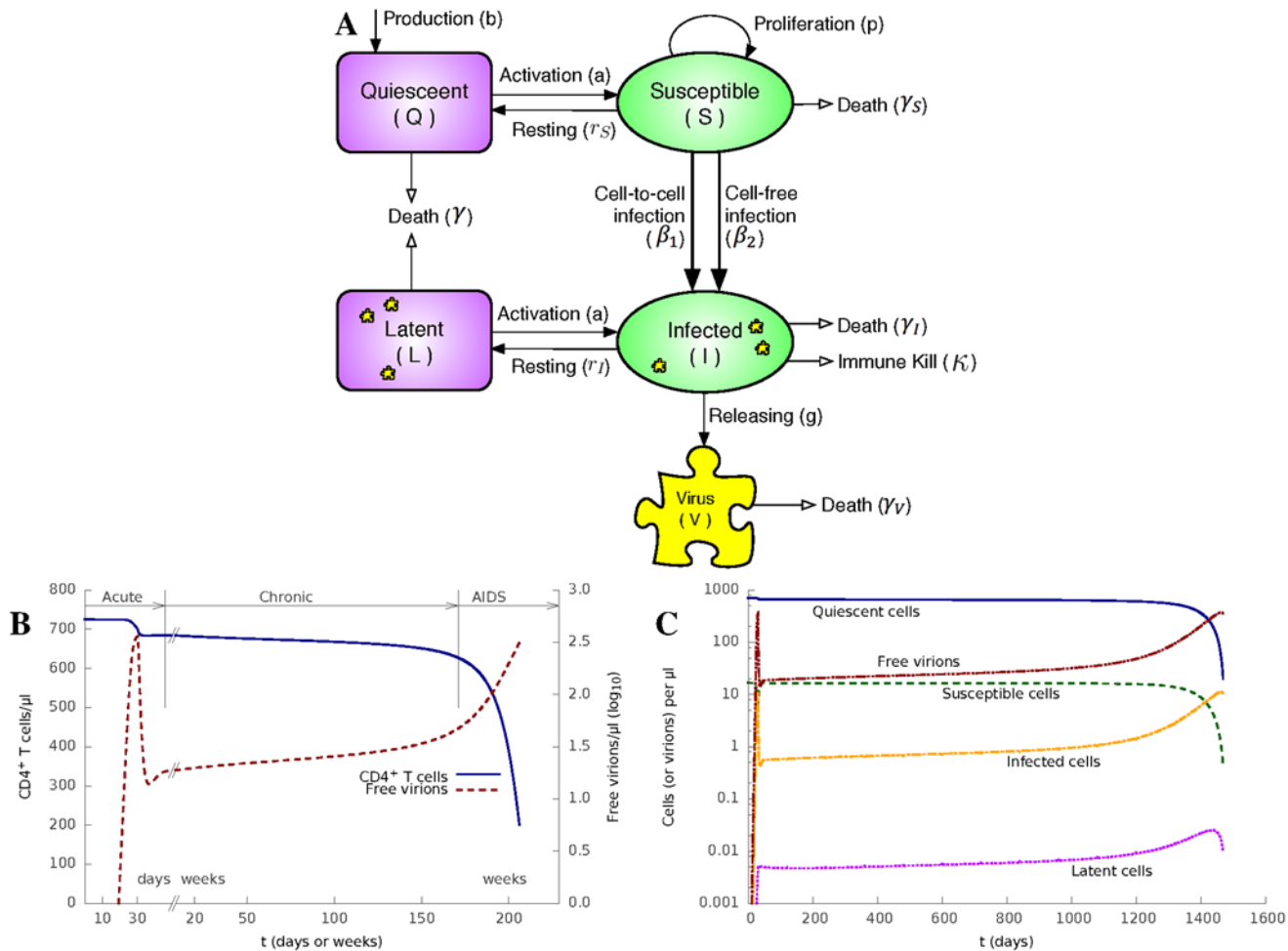
Fig 1. The HIV-1 model reproduces the full course of HIV-1 infection. (A) Diagrammatic representation of the model described by Equation 1.
(B) Numerical solutions of the model, plotting N, the density of all CD4$^+$ T cells (y axis on the left) and V, the density of free virions (y axis on the right in log scale) as a function of time (in days or weeks), respectively. The initial infection starts on day 0 and the cellular immune response starts on day 30. Parameter values are in Table 1.**(C)** The density of quiescent, susceptible, latent and infected CD4$^+$ T cells, and the density of free virions as function of time (in days).

doi:10.1371/journal.pcbi.1004179.g001

or virions drops to such low level, there is a high probability that it would die out (density becomes zero). The default value of parameters, shown in Table 1, are taken from the literature or estimated from clinical and experimentally observed data. The killing coefficient κ equals to its value in Table 1 when $t \geq D$; otherwise $\kappa = 0$ when $t < D$.

The production rate of new quiescent T cells from sources, such as thymus, within the human body is represented by b. Quiescent T cells are activated and become susceptible at a variable activation rate $a(N_M/N)$, where a is the activation coefficient and N_M is the density of T cells at which proliferation stops. The activation rate $a(N_M/N)$ increases as the total T cell density (N) falls (caused by the HIV-1 progression). The detailed mechanism of how the activation rate increases with the progression of HIV-1 is still unclear, and may include increased rates of co-infections, danger signals from dying T cells or homeostatic regulatory loops. This term, $a(N_M/N)$, here is an approximation, which encompasses the combined effects of all these different mechanisms. Quiescent T cells die at a rate of γ.

Table 1. Variables and parameters of our model.

	Variables	Initial value	Unit	
Q	Density of quiescent CD4$^+$ T cells [a]	$Q_0 = 708$	cells/µl	
S	Density of susceptible CD4$^+$ T cells [a]	$S_0 = 17$	cells/µl	
I	Density of infected CD4$^+$ T cells	$I_0 = 0$	cells/µl	
L	Density of latent CD4$^+$ T cells	$L_0 = 0$	cells/µl	
N	Density of all CD4$^+$ T cells	$N_0 = 725$	cells/µl	
V	Density of free HIV-1 virus	$V_0 = 10^{-6}$	virions/µl	
	Parameters	Default value	Unit	Reference
γ	Death rate of quiescent and latent cells	0.001	/day	[29]
γ_S	Death rate of susceptible cells	0.0625	/day	[30]
γ_I	Death rate of infected cells	0.5	/day	[29]
b	Production rate of new quiescent cells [b]	0.17	cells/µl/day	[31]
r_S	Resting rate of susceptible cells	0.5	/day	
r_I	Resting rate of infected cells	0.0001	/day	
a	Cell activation coefficient	0.01	/day	
p	Cell proliferation coefficient	1	/day	[29]
N_M	Cell threshold density [c]	800	cells/µl	
g	Virus release rate from an infected cell	100	virions/cell/day	[29]
γ_V	Virus death rate	3	/day	[29, 31]
c	Cell contact rate [d]	330	/day	[14, 32, 33]
θ	Cell synapse rate [e]	0.56		[12, 14, 32, 34]
β_1	Cell-to-cell infection rate [f]	0.19		[15, 33, 35, 36]
β_2	Cell-free infection rate	0.00135	µl/virions/day	[29]
D	Immune response delay [g]	30	days	[37]
κ	Killing coefficient (when $t \geqslant D$) [h]	1.5	/day	

[a] Q_0 and S_0 are chosen to maintain a stable density of CD4$^+$ T cells ($N_0 = 725$ cell/µl) in the absence of an infection;

[b] Production from sources including thymus;

[c] Beyond this threshold CD4$^+$ T cell proliferation stops;

[d] The average number of effective contacts between two CD4$^+$ T cells. Cells contact each other frequently, but only a proportion (20–25%) of these random contacts are sufficiently stable and "effective" for a synapse to be formed at rate θ;

[e] The average probability to form a virological synapse when two cells have an effective contact;

[f] The average probability that a susceptible cell is infected when it forms a synapse with an infected cell;

[g] Between the initial infection and the onset of cellular immune response, including the period before symptoms begin;

[h] $\kappa = 0$ when $t < D$.

Susceptible T cells turn into quiescent T cells at a rate r. They proliferate at a variable rate $p(1 − N/N_M)$, where p is the proliferation coefficient, N is the total T cell density, and N_M is the T cell density at which proliferation stops. This variable proliferation rate is a reasonable approximation [29] to the real T cell proliferation process, based on evidence [2] that T cell proliferation rate is density-dependent and would slow as the T cell density becomes high. Susceptible T cells die at a rate γ_S.

Susceptible T cells become infected through both cell-to-cell and cell-free infection. For cell-free infection, the number of newly infected T cells per unit period of time is $\beta_2 SV$, where β_2 is the infection rate of susceptible T cells by free virus. For cell-to-cell infection, we consider that the T cells are randomly moving, i.e. a T cell has an equal chance of contacting any other T cells. Let c represent the number of effective contacts each T cell makes in a unit period of time.

Then the number of contacts made by all infected T cells per unit period of time is cI. Among those contacts, S/N are contacts with a susceptible T cell that could potentially end up with a new infection. Let θ represent the Synapse rate: the average probability that two T cells form a virological synapse once they have made an effective contact. Then the number of newly infected T cells through cell-to-cell infection per unit time period can be represented as $cI(S/N)\theta\beta_1$, where β_1 is the cell-to-cell infection rate when an infected T cell and a susceptible T cell form a synapse. In reality, cell-to-cell transfer occurs locally involving only the infected cell and its immediate neighbours. The model abstracts this process by averaging infection over all cells. In practice, local effects will only distort this average when target cells in the vicinity of an infected cell become limiting. This limit seems unlikely to be reached except very late in infection, given that infected cells continue to migrate, albeit at a slower rate (personal observations and [17]), and uninfected target cells continue to migrate into the vicinity of an infected cell. More complex spatial models will be required, however, to understand the detailed anatomical distribution of HIV-1 infected cells over time. The amount of cell-to-cell transfer in the model depends on the number of infected T cells I and the proportion of susceptible cells S/N at any given time. Since N, the total density of CD4$^+$ cells, is not held constant, but in fact declines over time, cell-to-cell spread becomes increasingly effective as HIV-1 progresses.

The model does not explicitly distinguish antigen-presenting cell to T cell (APC/T) from T cell to T cell (T/T) transmission. APC/T transmission may potentially be most important very early in establishing infection [38], a process which is not examined in detail in this model. These two types of transmission are in fact both likely to occur most frequently and efficiently in the microenvironment of an APC/T cluster, where APC/T interactions lead to T cell activation, and hence favour also T/T interaction. Furthermore, there are very few quantitative estimates of the parameters of APC/T interaction in vivo. The incorporation of an additional cell type is therefore unlikely to have a major effect on the model behaviour, but would add significantly to model complexity and uncertainty.

The cause of T cell death in HIV-1 infection continues to be controversial, and probably includes several effects including lysis of infected cells by effector cells such as CD8 T cells and NK cells, apoptosis/pyroptosis and bystander death [27]. Non-immunological death of infected T cells is represented by a death rate of γ_I. And we use the term $\kappa \frac{I}{I+0.1} \frac{N}{N_M}$ to model the death of infected T cells by the cellular immune response. κ is initially 0 and changes to a higher value in Table 1 when the cellular immune response kicks in D (default value: 30) days after the initial infection. The term $\frac{I}{I+0.1}$ captures the relationship between the strength of the immune response and the density of infected CD4$^+$ T cells [8]. The term N/N_M captures immune exhaustion caused by HIV-1 infection. It falls from around 1 before infection towards 0 as HIV-1 progresses (because N_M is a constant and N, the total density of CD4$^+$ T cells, gradually declines with the HIV-1 progression).

Infected cells return to a quiescent state, and become latent, at rate r_I. Latent cells die and are activated (i.e. becomes infected cells) at the same rates as quiescent cells. Infected T cells release free viruses at rate g. Free viruses die at a rate of γ_V.

The abortive infection of quiescent cells is not considered in this simplified model, similarly to most previous modelling studies [1, 3, 39, 40]. HIV-1 immune escape mutants [41] are not directly modelled in this paper but their effects on degrading cellular immune response are reflected in the immune exhaustion in our model.

The numerical solutions of each of the variables are shown in Fig. 1C. Fig. 1B shows the combined CD4$^+$ T cell counts (N) and virus load (V), which are measured routinely in the clinic to monitor HIV-1 infection. Notably, the qualitative behaviour of the model accurately reflects the three main phases of disease that are observed clinically. The model reproduces an

acute infection phase, where the virus replicates rapidly (reflecting the absence of any pre-existing adaptive immunity), peaks and then returns to a low level by approximately 5 weeks. This metastable level of virus represents the clinical "set-point". Virus then remains stable for a prolonged period (note interruption and change of scale in x axis), during which time T cells decline very slowly. Finally, T cell numbers start to drop faster, and viral loads rise. The model calculation is stopped when CD4$^+$ level reaches 200 $cells/\mu l$.

It is important to note that the term $cI(S/N)\theta\beta_1$ we introduced for cell-to-cell spread is mathematically different from the classic term $\beta_2 SV$ which captures cell-free spread. N, the total CD4$^+$ number, is not a constant but decreases as a function of time. Indeed, if N in the cell-to-cell spread term is fixed, disease progression is not observed in the model (S1 Fig). Furthermore, N cannot be expressed as a simple function of V. In Fig. 1B the same value of V (free virion density) on each side of its peak around $t = 30$ days corresponds to two different N (CD4$^+$ T cell density) values. In addition, I, the number of infected cells, is not always proportional to V, especially early in infection (S2 Fig). Thus the term for cell-to-cell spread $cI(S/N)$ $\theta\beta_1$ shows different dynamics from the classic cell-free term $\beta_2 SV$.

Model evaluation

Most of the parameters of our model, and especially those determining HIV infectivity via cell-to-cell or cell-free spreading, were obtained from experimental observations (Table 1). It was therefore important to test that the model with this parametrization accurately fits real clinical data sets. We therefore evaluated our model against a set of longitudinal T cell count and virus load measurements obtained from a cohort of HIV-1-infected individuals who were recruited following clinical presentation with symptomatic acute HIV-1 infection and followed over time with serial measurement of plasma viral RNA levels and circulating T cell counts. The subjects selected for inclusion in this study all chose not to receive antiretroviral treatment in acute or early infection, and remained untreated until progression towards AIDS, evidenced by a substantial decline in their circulating CD4$^+$ T cell count (See Materials and Methods).

We use our model to theoretically reproduce the HIV-1 infection courses in the data. The values for HIV infectivity were fixed, as derived from the literature or our own observations (Table 1). Values for five parameters (Q_0, S_0, N_M, κ and D) describing the characteristics of the immune response were chosen for each patient to minimise the error of the predicted quasi-stable level of T cell counts (N_s) and viral load (V_s), and the time of progression to AIDS (t_A). All other values remained fixed at the default values in Table 1. The predicted progression results are compared against the actual measurements in Fig. 2 and S2 Table. The predicted V_s and t_A for each patient were negatively correlated (correlation coefficient = −0.46), in agreement with the well-established relationship between these two clinical values. Remarkably, the model can fit all patients by modifying the five immune-relevant parameters over a narrow range. Furthermore, the parameter values which gave the best results for the patients (see S1 Table) are all very close to those in Table 1, which were derived independently from experimental measurements.

The importance of cell-to-cell spread and cellular activation

Having confirmed that the model gives realistic estimations and predictions of real clinical data, we investigated the behaviour of the model in more detail. The role of the two spreading routes was further examined by systematic variation of the cell-to-cell infection rate, β_1, and the cell-free infection rate, β_2. The predicted outcome of infection are shown in Fig. 3. When either route is abolished, infection is blocked completely; T cell level returns to normal and virus is cleared after the cellular immune response kicks in. If cell-to-cell spread is removed from the
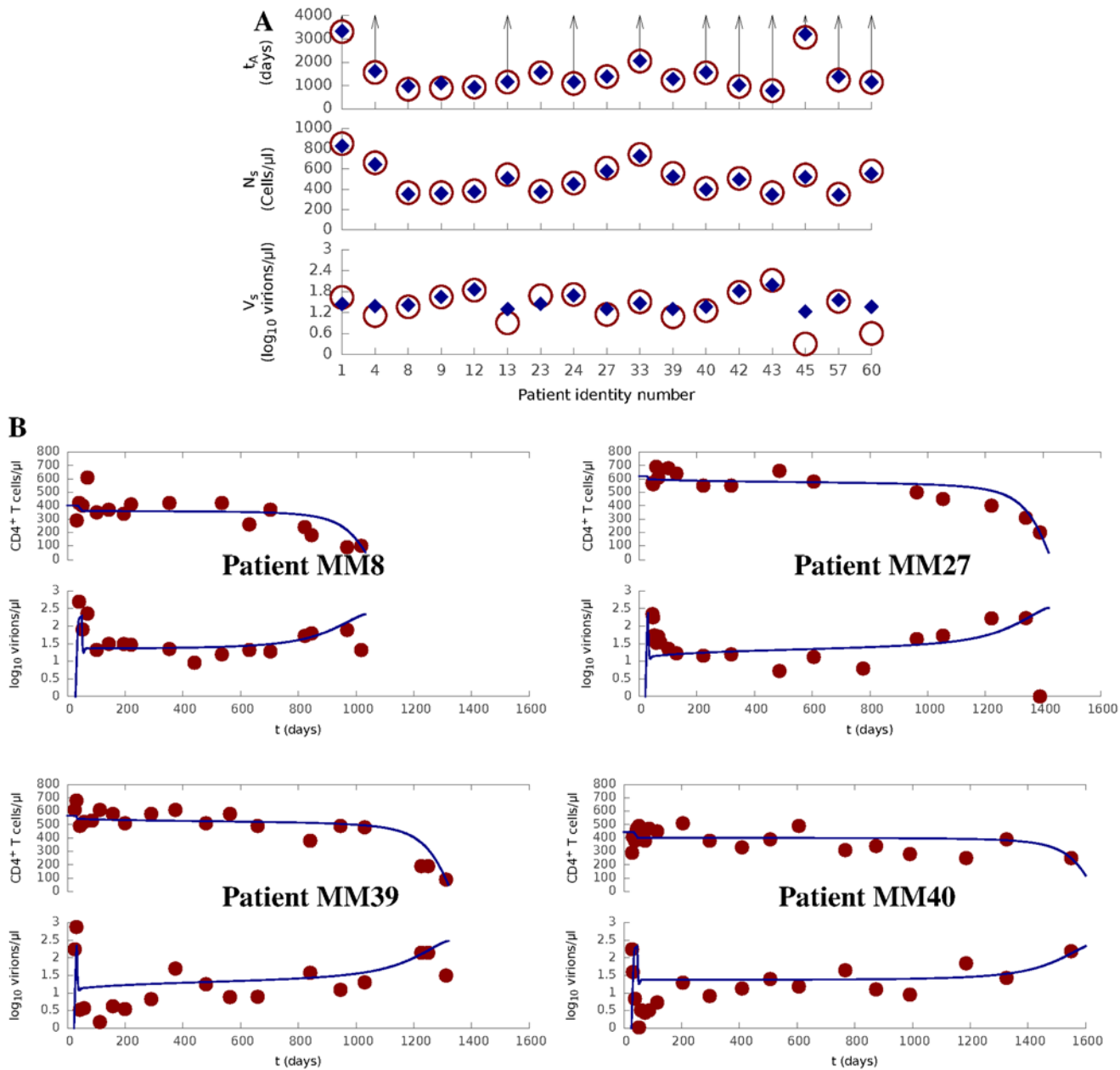
Fig 2. Model prediction for a cohort of treatment-naive HIV-1 patients. (A) Clinical data (circle and arrow) for all patients under study comparing against model prediction (diamond) for the time to AIDS (t_A), the quasi-steady density of CD4$^+$ T cells (N_s) and the quasi-steady density of free virions (V_s). An arrow represents that t_A is greater than a particular value (represented by the connected circle) for a patient as his / her CD4$^+$ count did not reached AIDS level (200 cells/μl) in the data.**(B)** Prediction (curve) of HIV progression course (N and $log_{10} V$) for four typical patients, where clinical data are shown as dots.Full prediction results are shown in S1 Table and S2 Table.

doi:10.1371/journal.pcbi.1004179.g002
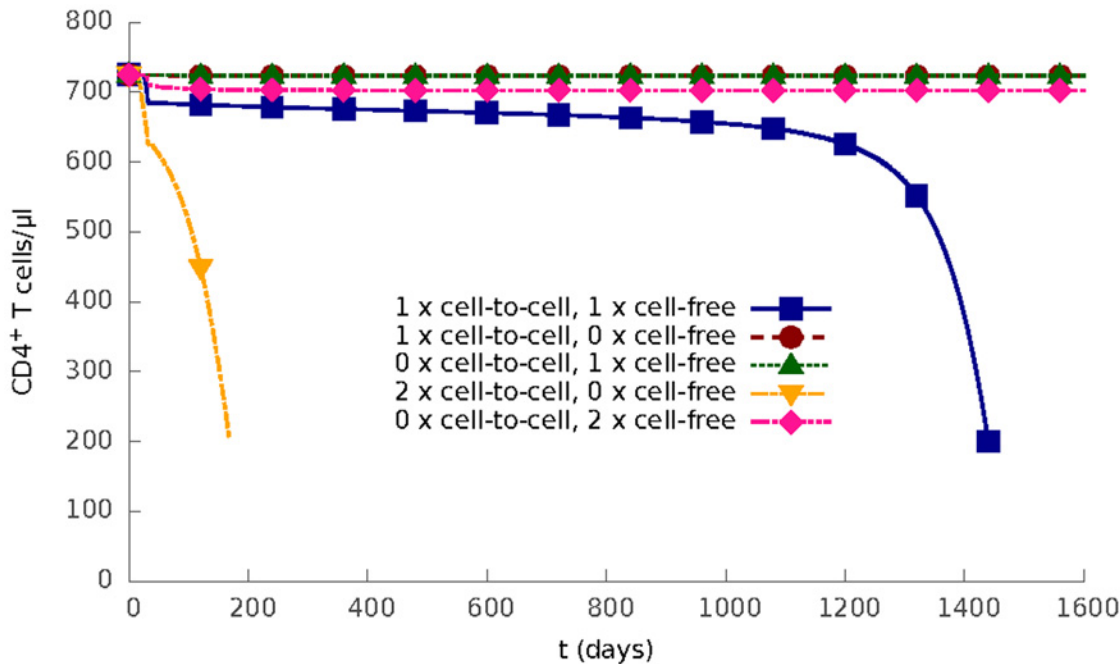
Fig 3. Two modes of HIV-1 infection. The density of CD4$^+$ T cells as a function of time for different values of cell-to-cell infection rate β_1 and cell-free infection rate β_2: (1) both use their default value, (2) β_1 uses its default value and $\beta_2 = 0$, (3) $\beta_1 = 0$ and β_2 uses its default value, (4) β_1 is twice its default value and $\beta_2 = 0$, (5) $\beta_1 = 0$ and β_2 is twice its default value.

doi:10.1371/journal.pcbi.1004179.g003

model ($\beta_1 = 0$) even a doubling in cell-free infection rate does not result in infection progression. In contrast, a doubling of cell-to-cell infection rate increases the set-point of viral load, and greatly speeds up the progression of infection even in the absence of cell-free infectivity. Thus the model suggests cell-to-cell spread may be an important force in allowing virus to establish infection in lymphoid tissue [38].

In the context of the model, the transition from phase 1 (acute) to phase 2 (stable chronic) is driven by a balance between several processes, including viral spreading through two parallel modes, and the cellular immune response, i.e. killing of infected cells as the cytotoxic CD8$^+$ T cell response becomes active. Paradoxically, in the stable chronic phase, the activation of T cells, which is the hallmark of adaptive immunity and is aimed at protecting the host, in fact contributes to the persistence of HIV-1. The role of CD4$^+$ T cell activation is explored in Fig. 4A. In this model, the rate of T cell activation $a(N_M/N)$ increases as the number (N) of T cells falls, which can be considered to represent a type of homeostatic regulation reinforcing immunological activity relevant to the progressive damage of the immune system and its consequences. In the absence of this feedback (i.e. when activation rate is fixed), HIV infection would not progress to AIDS after the onset of the cellular immune response. In contrast, if the activation rate is doubled, then infection progresses significantly faster to AIDS. These results confirm and extend the findings of DeBoer and Perelson [29], which suggested an increasing rate of cellular activation was important in establishment of chronic infection and progression to AIDS. The results are also consistent with evidence that non-pathogenic SIV infection in the natural host species results in viral replication in the absence of chronic immune activation and no AIDS [42]. Fig. 4B depicts the number of CD4$^+$ T cells newly infected via either cell-to-cell spread or cell-free spread as the infection progresses. The model predicts that cell-to-cell
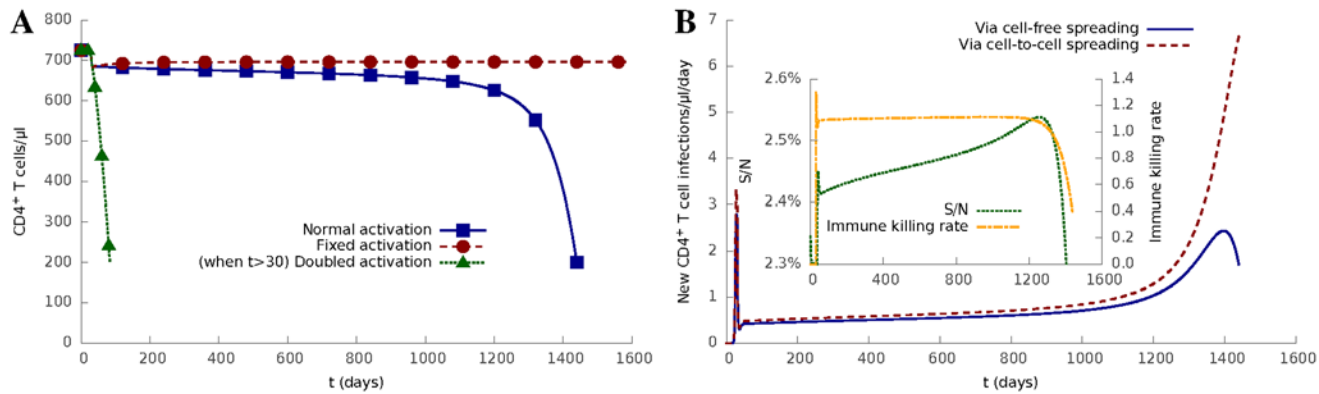
Fig 4. Progressive CD4+ T cell activation drives progression to AIDS and increased cell-to-cell infection. (A) Progression of HIV-1 infection for different cell activation rates, including (1) normal activation (aN_M/N in Equation 1), (2) fixed activation (aN_M/N_0, where N_0 is the initial density of CD4+ T cells), and (3) doubled activation ($2 \times aN_M/N$ when $t > D$).**(B)** Numbers of newly infected cells in a day via cell-to-cell spreading and cell-free spreading, respectively. The inset shows the ratio of susceptible cells to all cells (S/N, left y axis) and the strength of immune response ($\kappa \frac{I}{I+0.1} \frac{N}{N_M}$, right y axis) as a function of time, respectively.

doi:10.1371/journal.pcbi.1004179.g004

transfer becomes increasingly dominant as the total number of CD4+ T cells falls, the proportion of susceptible cells rises (Fig. 4B inset left y axis) and the strength of immune response falls (because of immune exhaustion, see Fig. 4B inset right y axis).

Treatment evaluation

Modelling can help evaluate the long term effects of different treatments on HIV-1 progression. Once the start time, duration, and effectiveness against two modes of HIV-1 spread are known for a treatment, its effects on HIV-1 progression can be evaluated by the model.

To validate the model's ability to evaluate HIV-1 treatments, we use it to theoretically reproduce the results of the Short Pulse Anti-Retroviral Therapy at Seroconversion (SPARTAC) trial [28]. The SPARTAC trial aims to evaluate how the short-course antiretroviral therapy (ART) delays HIV progression. The patients (366 in total) who participated in the trial were randomly assigned to three groups: standard care, 12-week ART treatment, and 48-week ART treatment. For these three groups of patients, the primary end point t_p (defined as when CD4+ count ≤ 350 $cells/\mu l$ or the start of long-term ART) on average reached 157 weeks (standard care), 184 weeks (12-week ART), and 222 weeks (48-week ART) after randomisation. Randomisation is the time when the trial starts.

We first estimate the trial time points (randomisation, start of the treatments, and primary end points t_p) in terms of days after the initial infection (See Materials and Methods). We then use the average CD4+ count and virus load of all patients at randomisation, and the primary end point of the patients in standard care group to fit the five immune-relevant model parameters (Q_0, S_0, N_M, κ and D). These fitted parameters represent an average patient in the trial.

We then evaluated the effects of 12 and 48 week therapy using the model. We assumed that the therapy was 100% effective against cell-free transmission, but we evaluated the model for both 100% and 50% efficiency against cell-to-cell transmission, since cell-to-cell transmission has been reported as being more resistant to some forms of therapy [43, 44]. Both modalities reproduced the observed effects of therapy well, and the model results were robust to changes in the efficiency (Table 2). The model therefore not only fits known data sets (standard care

Table 2. Model prediction of the SPARTAC trial.

Patient groups:		Standard-care	12-week-treatment	48-week-treatment
N_r (cells/µl)	Data:	559		
	Model:	560		
V_r (virons/µl)	Data:	17 ($log_{10} V_r = 1.2$)		
	Model:	12 ($log_{10} V_r = 1.1$)		
t_p (days)	Data:	1,197	1,386	1,652
	Model:	1,197	**1,392** | 1,394	**1,654** | 1,656

N_r and V_r are the density of CD4$^+$ T cells and free virions at *randomisation* (when patients groups are randomly divided and the trial starts). t_p is the time between the initial infection and the *primary end point* (when density of CD4$^+$ T cells decreases to 350 *cells/µl* or the start of long-term ART [28]). The t_p estimated from the model is the time when CD4$^+$ T cells decreases to 350 *cells/µl*. The Materials and Methods section describes how t_p is inferred from the data [28] in terms of days after infection. The model parameters calibrated from the trial data (by fitting the average N_r, V_r for all patients and t_p for the standard care group) are $Q_0 = 566$ *cells/µl*, $S_0 = 13$ *cells/µl*, $N_M = 638$ *cells/µl*, $\kappa = 1.292165$ */day* and $D = 28$ *days*. The model predictions use the same Nr and Vr for all three patient groups, which are the average of all patients in the trial. The trial treatment is assumed to be 100% effective against cell-free HIV-1 spread. We estimate the t_p for 12-week and 48-week treatment groups if the treatment is 50% (value in bold font) or 100% (value in normal font) effective against cell-to-cell spread of HIV-1.

group) but also accurately predicts the effects of new treatment regimes on two independent patient groups (12-week and 48-week).

We therefore further explored the sensitivity of the model to perturbation as a function of treatment starting time (Fig. 5). The "treatment" lasts for 30 days, during which both cell-free and cell-to-cell infection are completely blocked. Once "treatment" is finished, two modes of HIV-1 infection resume. Early treatment in this model (3 days after infection, i.e. post-
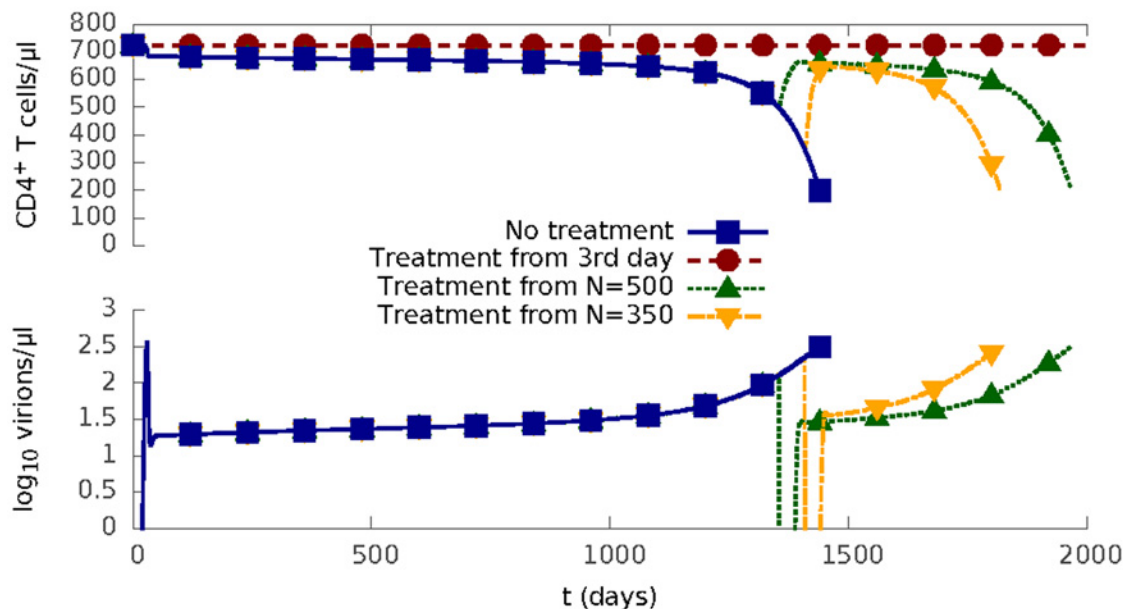
Fig 5. Impact of treatment starting time on HIV progression. HIV progression for a 30-day 'perfect' treatment starting at three different times after the initial infection: (1) on the 3rd day when the density of all CD4$^+$ T cells is $N = 725$ *cells/µl*, (2) when $N = 500$ *cells/µl*; (3) when $N = 350$ *cells/µl*. The 'prefect' treatment here means both cell-to-cell infection and the cell-free infection are completely blocked (i.e. $\beta_1 = 0$, $\beta_2 = 0$ and the virus release rate $g = 0$) for 30 days.
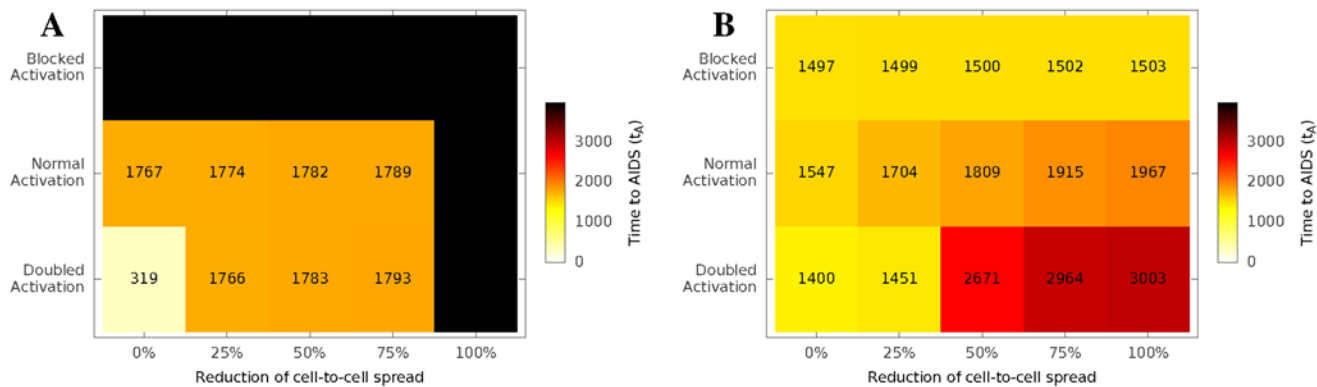
Fig 6. Prediction of the time to AIDS, t_A, for different treatment schemes. We consider 30-day treatments starting **(A)** on the 3rd day and **(B)** when $N = 500$ *cells/µl*, respectively. All treatments block cell-free infection completely ($\beta_2 = 0$ and $g = 0$). The treatments also affect cell-to-cell infection (x axis) and / or manipulate the CD4$^+$ T cell activation process (y axis, see Fig. 4A). The black squares represent treatments that reduced the density of infected cells, latent cells and free virions all below 10^{-12} per *µl*.

exposure prophylaxis) leads to no decline in CD4$^+$ T cell density, and no chronic infection phase. The same treatment applied when T cell density reaches the levels (500 CD4$^+$ T *cells/µl* and 350 CD4$^+$ T *cells/µl*) at which the World Health Organization recommends ART initiation [45] is followed by a rapid virus rebound after the treatment stops, and the disease progresses according to its normal course. Thus, as HIV-1 progresses it becomes increasingly difficult to control infection in this model.

Finally, we looked at the interactions between treatment starting time, activation rate and efficiency of therapy against cell-to-cell spread (Fig. 6). In general, increased efficiency of therapy and earlier treatment both prolonged time to progression to AIDS. However, the effects of altered activation depend in a complex way on the context of the intervention. Blocking activation early is beneficial, since it will reduce the number of susceptible cells HIV-1 can infect; while blocking activation late, when the latent HIV-1 reservoir has been established, will prevent latent HIV-1 from being activated and eradicated. Increasing cellular activation, which has been proposed as a means of flushing out the latent reservoir [46], can be effective in increasing time to AIDS when given in the context of efficient anti-viral therapy, but can shorten the time if concomitant anti-viral therapy is incomplete. This is because increasing cellular activation increases both the number of susceptible cells (activated from quiescent cells) and the number of infected cells (activated from latent cells) at the same time. Thus if it is used together with an effective anti-viral therapy, the latent HIV-1 reservoir will be flushed out and killed by the antiviral drugs. But if the concomitant anti-viral therapy is not efficient enough to clear the increased number of infected cells, the spread of HIV-1 will speed up.

Discussion

The aim of this study was to develop a model that reduces the enormous biological complexity of the course of HIV-1 infection to a few well-defined equations but nevertheless retains the main dynamic features of the disease. In particular, the model was required to predict the evolution of a long lived metastable state of low level viral infection, which ultimately breaks down to uncontrolled viral growth and a precipitous fall in CD4$^+$ T cells, two hallmarks of AIDS. The model incorporates both an immune response, which is believed to be a major factor limiting viral expansion by killing of infected cells, and the formation of long lived latently infected cells, which are believed to play an important role in limiting the long-term effects of antiviral therapy. The key distinguishing features of the model are that it incorporates explicitly

cell-to-cell spread of virus as well as classical spread via cell-free virus. The motivation of building such a model was to investigate the role of these two modes of spread in determining the outcome of infection, and thus complement the limited *in vivo* experimental and clinical data available addressing this question.

A fundamental prediction of the model is that, given the known experimentally derived parameters of cell-to-cell and cell-free spreading, the two modes of spread complement each other and both make important contributions to disease progression. In addition, it is clear that there is a close relationship between the proportion of activated T cells, cell-to-cell spread and disease progression. Specifically, cell-to-cell spreading is strong when the percentage of activated, and therefore susceptible cells is high in the population, since an infected cell is then more likely to encounter an effective target (a susceptible cell) to infect. When the percentage of susceptible cells is low, infected cells will mostly encounter quiescent/resting cells that will provide ineffective targets. These conditions may occur both early and late in HIV-1 infection. The site of infection itself (for example the vaginal mucosa) may contain a large proportion of activated T cells some of which may be interacting with APC, particularly if there is a concomitant sexually transmitted infection. The well-documented association between HIV-1 infection and other mucosal infections may therefore reflect the key importance of a high concentration of APC and activated T cells in early transmission of virus [47]. There is also convincing evidence that gut associated lymphoid tissue is a major site of viral replication early on in disease [48, 49]. This tissue is characterized by an unusually large proportion of T cells capable of supporting HIV-1 replication, presumed to result from chronic exposure to the gut microbiome. Since cell-to-cell spread is much more efficient, and under these conditions the number of activated target cells are not limiting, our model predicts that gut lymphoid tissue would provide an ideal microenvironment for rapid propagation of HIV-1, at least until the majority of target cells are infected or die. Further development of the basic model, to allow heterogeneity associated with different anatomical compartments would allow this prediction to be tested directly.

The model also predicts a dominant role for cell-to-cell spread in the late phase of HIV-1. As in the scenario early in infection in the gut lymphoid tissue, our model predicts that late stage disease will be associated with a large number of infected cells, combined with a large proportion of activated target cells. A high number of infected cells is a simple corollary of the very high levels of free virus late in infection in the absence of treatment. There is also substantial experimental evidence for increased immune activation in the late phases of HIV-1 [26], and indeed this has been proposed as an important contribution to pathogenesis. Thus cell-to-cell spread is likely to become the dominant mode of transmission in the late stages of HIV-1. This may be important in light of recent data showing that the different components of current HAART display variable efficacy against cell-to-cell spread [43, 44].

Interestingly, the hybrid spreading mechanism employed by HIV-1 is reminiscent of those of some computer worms such as Red Code II and Cornficker [20, 21], which allocate their resources between probing for susceptible target computers in local area networks and globally across the internet. Similarly to HIV-1, local interactions have a high chance of success but access only a limited number of targets while global spread targets a much larger number of targets with a much lower probability of success. Modelling studies have shown that this hybrid spreading is required to explain the large outbreak of such worms on the Internet [25]. It is tempting to speculate that hybrid spreading may contribute to the pathogenicity and dynamics of infection of other viruses that employ parrallel spreading mechanisms, for example Hepatitis C virus [19].

The current model incorporates some simplifying assumptions. Nevertheless, the model does provide some insights into the effectiveness of therapy at different stages of disease. Specifically, the model strongly supports the hypothesis that interfering with viral infection early in HIV-1 progression is likely to have a major impact on the subsequent progress of the disease.

Interfering with viral transmission is predicted by our model to be much more effective early in HIV-1 infection. The clinical decision about when to start therapy remains a matter of debate. Current WHO guidelines suggest commencing treatment at CD4$^+$ T cell density of $>$ 350$cells/\mu l$ and $<$ 500$cells/\mu l$ [45]. However, studies exploring much earlier commencements of treatment, have claimed increased efficacy [28, 50]. For example, the recent "Short Pulse Anti-Retroviral Therapy at Seroconversion" (SPARTAC) trial, demonstrated a long term clinical benefit of a limited period of ART soon after seroconversion [28]. Our model accurately predicted the results of the SPARTAC trial providing further support for the model's generality and robustness.

Anti-viral therapies that specifically target cell-to-cell spread are not currently available, but are clearly important therapeutic goals [44]. A number of previous studies have proposed combining antiviral therapies with therapies that either limit CD4+ T cell activation (thus reducing the number of target susceptible cells) or increased T cell activation, thus flushing out residual latent cells. These approaches have not given clear cut clinical benefits [51, 52]. Indeed our model suggests that the outcome of such manipulation of cellular activation will be critically dependent on the time at which it is administered, and the efficiency of concomitant antiviral therapy. Targeted suppression of CD4$^+$ T cell activation, in combination with antiviral therapies may nevertheless offer a useful approach, if used early on in infection.

Mathematical models provide an important tool for understanding and predicting the course of natural HIV-1 infection that complements clinical studies. The most appropriate therapeutic regimens for HIV therapy continue to remain the subject of disagreement and debate. In addition, many new therapeutic modalities aimed at achieving viral eradication, such as the HDAC inhibitors [46], or therapeutic vaccination [53] are being proposed. However, testing new treatment regimens is a costly and time consuming task, and the logistic challenges and expense of running clinical trials to evaluate and compare treatments remain a major bottleneck to translational advances in HIV therapy. Mathematical models have proved of value in the past, but have suffered from omitting important biological processes, thus compromising their ability to accurately recapitulate clinical observations. Our model explicitly incorporates cell-to-cell transmission, and changing rates of cellular activation, two processes that are known to be a key feature of HIV infection. With increased sophistication, and hence ability to accurately model the known biological drivers of disease progression, mathematical models can become increasingly important in preclinical testing of modified or novel HIV therapies. The model developed here provides specific predictions which emerge from the close links between CD4$^+$ T cell activation and cell-to-cell spread, and their combined contribution to both early and late phases of HIV-1. These predictions emphasize the potential benefits of early or prophylactic treatment with antiretroviral therapies, and suggest that drugs with the ability to effectively block cell-to-cell spread may provide significant therapeutic benefit in long term management or eradication of HIV-1 infection.

Materials and Methods

Recruitment and follow-up of HIV-1 infected patients (London data)

Individuals acutely-infected with HIV-1 were recruited at the Mortimer Market Centre for Sexual Health and HIV Research (London, UK). Subjects were mostly male Caucasians who presented with symptoms of acute retroviral illness. Patient viral loads and CD4$^+$ T cell counts were measured longitudinally at serial time-points following infection using standard clinical tests. All subjects were offered anti-retroviral treatment at diagnosis. The subjects selected for inclusion in the study all chose not to receive anti-retroviral therapy in acute or early infection,

and remained untreated until disease progression, evidenced by a substantial decline in their circulating CD4$^+$ T cell count occurred.

Ethics statement

Patients provided written informed consent for study participation. Study approval was obtained from The National Health Service Camden and Islington Community Local Research Ethics Committee.

Selection of patients to be included in the study (London data)

There were 39 patients in total in the data from Mortimer Market Centre for Sexual Health and HIV Research (London, UK). For this study, we focused our analysis only on patients with more than ten data points for both HIV load and CD4$^+$ measurements (29 out of the 39 patients). We also excluded from the analysis a further 12 patients who showed no overall decrease in CD4$^+$ count, or no increase in viral load at later timepoints. The focus of the model described above is to capture the "typical" characteristics of HIV infection, which include that CD4$^+$ count falls in general, and viral load increases in general as infection progresses. It is widely accepted that in some patients (for example the so-called "elite controllers") viral load remains low or undetectable and CD4$^+$ count remains unchanged for long periods. The mechanisms responsible for these phenomena are still incompletely understood. The current model does not attempt to incorporate any such mechanism, and this group of patients was therefore not included in the study. Further elaboration of the current model to include additional features of viral control will be informative in helping to understand such patients. The identifiers for the remaining 17 patients are: MM1, MM4, MM8, MM9, MM12, MM13, MM23, MM24, MM27, MM33, MM39, MM40, MM42, MM43, MM45, MM57, MM60.

Estimation of the time points of the SPARTAC trial

According to [28], the median interval between seroconversion and randomization (start of trial) was 12 weeks. The exact average time of seroconversion for patients in the SPARTAC trial is not directly available from [28]. We assume it is 2 weeks after initial infection, as seroconversion normally happens within a few weeks after HIV-1 infection. Then the time of randomization (start of trial) can be estimated as $7(2 + 12) = 98$ *days* after infection. The treatment is estimated to start 3 days after randomization [28], i.e. $98 + 3 = 101$ *days* after infection. And the primary end points for patients in standard care, 12-week ART, and 48-week ART groups are respectively: $98 + 7 \times 157 = 1197$ *days*, $98 + 7 \times 184 = 1386$ *days*, and $98 + 7 \times 222 = 1652$ *days* after infection.

Availability and implementation

Calculation results in this paper are obtained using LeoTask [54], a parallel task running and results aggregation framework that we have developed for computational research. The framework and an executable programme that implements our HIV-1 model are both freely available at http://github.com/mleoking/leotaskapp.

Supporting Information

S1 Table. Model parameters calibrated from a cohort of treatment-naive HIV-1 patients. Results are shown for all 17 patients. In the data, time is recorded relative to the first appearance of symptoms of HIV infection. As the actual initial infection date is unknown, we

assumed a constant "eclipse" phase of 20 days between initial infection and first appearance of symptoms.
(PDF)

S2 Table. Model prediction of a cohort of treatment-naive HIV-1 patients. N_S is the quasi-steady CD4$^+$ T cell density and V_S is the quasi-steady density of free virions, which are average densities between the 100th and 800th days after initial infection. t_A is the time to AIDS, which is defined as the time between initial infection and when the density of CD4$^+$ T cells falls to 200 *cells/μl*.
(PDF)

S1 Fig. HIV-1 infection course generated by the HIV-1 model using two different cell-to-cell infection terms. 1) the normal cell-to-cell infection term ($c\theta\beta_1 IS/N$) in Equation 1, and 2) the cell-to-cell infection term that fixes N to be N_0 ($c\theta\beta_1 IS/N_0$ where N_0 is the total number of CD4$^+$ T cells before HIV-1 infection and it is a constant). With a fixed $N = N_0$ in the term, the HIV-1 model would not be able to recapitulate the AIDS phase.
(TIFF)

S2 Fig. *V/I* (density of free virions divided by the density of infected CD4$^+$ T cells) as a function of time. There are some obvious changes in *V/I* during the early days of HIV-1 infection. The figure however also supports some existing works' [8] assumption that *V* and *I* are proportional to each other during the chronic (stable) phrase of HIV-1 infection. Our model depicts HIV-1 infection in all its three phrases and we do not therefore assume *V* to be proportional to *I*.
(TIFF)

Acknowledgments

Author Contributions

References

1. Perelson AS, Ribeiro RM (2013) Modeling the within-host dynamics of hiv infection. BMC Biol 11: 96. doi: 10.1186/1741-7007-11-96 PMID: 24020860

2. Ho DD, Neumann AU, Perelson AS, Chen W, Leonard JM, et al. (1995) Rapid turnover of plasma virions and CD4 lymphocytes in HIV-1 infection. Nature 373: 123–126. doi: 10.1038/373123a0 PMID: 7816094

3. Perelson AS, Neumann AU, Markowitz M, Leonard JM, Ho DD (1996) Hiv-1 dynamics in vivo: Virion clearance rate, infected cell life-span, and viral generation time. Science 271: 1582–1586. doi: 10.1126/science.271.5255.1582 PMID: 8599114

4. Prague M, Commenges D, Thiebaut R (2013) Dynamical models of biomarkers and clinical progression for personalized medicine: The HIV context. Adv Drug Deliv Rev 65: 954–965. doi: 10.1016/j.addr.2013.04.004 PMID: 23603207

5. Xiao Y, Miao H, Tang S, Wu H (2013) Modeling antiretroviral drug responses for HIV-1 infected patients using differential equation models. Adv Drug Deliv Rev 65: 940–953. doi: 10.1016/j.addr.2013.04.005 PMID: 23603208

6. Alizon S, Magnus C (2012) Modelling the course of an HIV infection: Insights from ecology and evolution. Viruses 4: 1984–2013. doi: 10.3390/v4101984 PMID: 23202449

7. Elemans M, Florins A, Willems L, Asquith B (2014) Rates of CTL killing in persistent viral infection in vivo. PLoS Comput Biol 10: e1003534. doi: 10.1371/journal.pcbi.1003534

8. Deutekom HWMv, Wijnker G, Boer RJ (2013) The rate of immune escape vanishes when multiple immune responses control an HIV infection. J Immunol 191: 3277–3286. doi: 10.4049/jimmunol.1300962 PMID: 23940274

9. Rong L, Perelson AS (2009) Modeling latently infected cell activation: Viral and latent reservoir persistence, and viral blips in hiv-infected patients on potent therapy. PLoS Comput Biol 5: e1000533. doi: 10.1371/journal.pcbi.1000533

10. Spina CA, Anderson J, Archin NM, Bosque A, Chan J, et al. (2013) An in-depth comparison of latent HIV-1 reactivation in multiple cell model systems and resting CD4+ t cells from aviremic patients. PLoS Pathog 9: e1003834.

11. Sattentau Q (2008) Avoiding the void: cell-to-cell spread of human viruses. Nat Rev Microbiol 6: 815–826. doi: 10.1038/nrmicro1972 PMID: 18923409

12. Jolly C, Kashefi K, Hollinshead M, Sattentau QJ (2004) HIV-1 cell to cell transfer across an env-induced, actin-dependent synapse. J Exp Med 199: 283–293. doi: 10.1084/jem.20030648 PMID: 14734528

13. Komarova NL, Levy DN, Wodarz D (2013) Synaptic transmission and the susceptibility of HIV infection to anti-viral drugs. Sci Rep 3. doi: 10.1038/srep02103 PMID: 23811684

14. Martin N, Welsch S, Jolly C, Briggs JAG, Vaux D, et al. (2010) Virological synapse-mediated spread of human immunodeficiency virus type 1 between T cells is sensitive to entry inhibition. J Virol 84: 3516–3527. doi: 10.1128/JVI.02651-09 PMID: 20089656

15. Sourisseau M, Sol-Foulon N, Porrot F, Blanchet F, Schwartz O (2007) Inefficient human immunodeficiency virus replication in mobile lymphocytes. J Virol 81: 1000–1012. doi: 10.1128/JVI.01629-06 PMID: 17079292

16. Duncan CJA, Russell RA, Sattentau QJ (2013) High multiplicity HIV-1 cell-to-cell transmission from macrophages to CD4+ t cells limits antiretroviral efficacy. AIDS 27: 2201–2206. doi: 10.1097/QAD.0b013e3283632ec4 PMID: 24005480

17. Murooka TT, Deruaz M, Marangoni F, Vrbanac VD, Seung E, et al. (2012) HIV-infected T cells are migratory vehicles for viral dissemination. Nature 490: 283–287. doi: 10.1038/nature11398 PMID: 22854780

18. Sewald X, Gonzalez DG, Haberman AM, Mothes W (2012) In vivo imaging of virological synapses. Nat Commun 3: 1320. doi: 10.1038/ncomms2338 PMID: 23271654

19. Zeisel MB, Felmlee DJ, Baumert TF (2013) Hepatitis C virus entry. Curr Top Microbiol Immunol 369: 87–112. PMID: 23463198

20. Moore D, Shannon C, Claffy K (2002) Code-red: a case study on the spread and victims of an internet worm. In: Proceedings of ACM SIGCOMM Workshop on Internet measurment. ACM, pp. 273–284. doi:10.1145/637201.637244

21. Zhang C, Zhou S, Chain BM (2014). Hybrid epidemics - a case study on computer worm conficker. Preprint. Available: arXiv:1406.6046. Accessed 10 Feb 2015.

22. Wang P, Gonzalez MC, Hidalgo CA, Barabasi AL (2009) Understanding the spreading patterns of mobile phone viruses. Science 324: 1071–1076. doi: 10.1126/science.1167053 PMID: 19342553

23. Keeling MJ, Danon L, Vernon MC, House TA (2010) Individual identity and movement networks for disease metapopulations. Proc Natl Acad Sci USA 107: 8866–8870. doi: 10.1073/pnas.1000416107 PMID: 20421468

24. Balcan D, Vespignani A (2011) Phase transitions in contagion processes mediated by recurrent mobility patterns. Nat Phys 7: 581–586. doi: 10.1038/nphys1944 PMID: 21799702

25. Zhang C, Zhou S, Cox IJ, Chain BM (2014). Optimizing hybrid spreading in metapopulations. Preprint. Available: arXiv: 1409.7291. Accessed 10 Feb 2015.

26. Miedema F, Hazenberg MD, Tesselaar K, Baarle Dv, de Boer RJ, et al. (2013) Immune activation and collateral damage in AIDS pathogenesis. Front Immunol 4: 298. doi: 10.3389/fimmu.2013.00298 PMID: 24133492

27. Doitsh G, Galloway NLK, Geng X, Yang Z, Monroe KM, et al. (2014) Cell death by pyroptosis drives CD4 T-cell depletion in HIV-1 infection. Nature 505: 509–514. doi: 10.1038/nature12940 PMID: 24356306

28. Fidler S, Porter K, Ewings F, Frater J, Ramjee G, et al. (2013) Short-course antiretroviral therapy in primary HIV infection. N Engl J Med 368: 207–217. doi: 10.1056/NEJMoa1110039 PMID: 23323897

29. De Boer R, Perelson A (1998) Target cell limited and immune control models of HIV infection: A comparison. J Theor Biol 190: 201–214. doi: 10.1006/jtbi.1997.0548 PMID: 9514649

30. Mohri H, Perelson AS, Tung K, Ribeiro RM, Ramratnam B, et al. (2001) Increased turnover of T lympho-cytes in HIV-1 infection and its reduction by antiretroviral therapy. J Exp Med 194: 1277–1287. doi: 10.1084/jem.194.9.1277 PMID: 11696593

31. Stafford MA, Corey L, Cao Y, Daar ES, Ho DD, et al. (2000) Modeling plasma virus concentration during primary HIV infection. J Theor Biol 203: 285–301. doi: 10.1006/jtbi.2000.1076 PMID: 10716909

32. Jolly C, Mitar I, Sattentau QJ (2007) Requirement for an intact T-cell actin and tubulin cytoskeleton for efficient assembly and spread of human immunodeficiency virus type 1. J Virol 81: 5547–5560. doi: 10.1128/JVI.01469-06 PMID: 17360745

33. Jolly C, Booth NJ, Neil SJD (2010) Cell-cell spread of human immunodeficiency virus type 1 overcomes tetherin/bst-2-mediated restriction in T cells. J Virol 84: 12185–12199. doi: 10.1128/JVI.01447-10 PMID: 20861257

34. Hübner W, McNerney GP, Chen P, Dale BM, Gordon RE, et al. (2009) Quantitative 3D video microsco-py of HIV transfer across T cell virological synapses. Science 323: 1743–1747. doi: 10.1126/science.1167525

35. Chen P, Hübner W, Spinelli MA, Chen BK (2007) Predominant mode of human immunodeficiency virus transfer between T cells is mediated by sustained env-dependent neutralization-resistant virological synapses. J Virol 81: 12582–12595. doi: 10.1128/JVI.00381-07 PMID: 17728240

36. Del Portillo A, Tripodi J, Najfeld V, Wodarz D, Levy DN, et al. (2011) Multiploid inheritance of HIV-1 dur-ing cell-to-cell infection. J Virol 85: 7169–7176. doi: 10.1128/JVI.00231-11 PMID: 21543479

37. McMichael AJ, Borrow P, Tomaras GD, Goonetilleke N, Haynes BF (2010) The immune response dur-ing acute HIV-1 infection: clues for vaccine development. Nat Rev Immunol 10: 11–23. doi: 10.1038/nri2674 PMID: 20010788

38. Parrish NF, Gao F, Li H, Giorgi EE, Barbian HJ, et al. (2013) Phenotypic properties of transmitted found-er HIV-1. Proc Natl Acad Sci USA 110: 6626–6633. doi: 10.1073/pnas.1304288110 PMID: 23542380

39. Komarova NL, Wodarz D (2013) Virus dynamics in the presence of synaptic transmission. Math Biosci 242: 161–171. doi: 10.1016/j.mbs.2013.01.003 PMID: 23357287

40. Komarova NL, Anghelina D, Voznesensky I, Benjamin T, Levy DN, et al. (2013) Relative contribution of free-virus and synaptic transmission to the spread of HIV-1 through target cell populations. Biol Lett 9. doi: 10.1098/rsbl.2012.1049 PMID: 23269844

41. Fryer HR, Frater J, Duda A, Roberts MG, Phillips RE, et al. (2010) Modelling the evolution and spread of HIV immune escape mutants. PLoS Pathog 6: e1001196. doi: 10.1371/journal.ppat.1001196

42. Silvestri G, Paiardini M, Pandrea I, Lederman MM, Sodora DL (2007) Understanding the benign nature of SIV infection in natural hosts. J Clin Invest 117: 3148–3154. doi: 10.1172/JCI33034 PMID: 17975656

43. Sigal A, Kim JT, Balazs AB, Dekel E, Mayo A, et al. (2011) Cell-to-cell spread of HIV permits ongoing replication despite antiretroviral therapy. Nature 477: 95–98. doi: 10.1038/nature10347 PMID: 21849975

44. Titanji BK, Aasa-Chapman M, Pillay D, Jolly C (2013) Protease inhibitors effectively block cell-to-cell spread of HIV-1 between T cells. Retrovirology 10: 161. doi: 10.1186/1742-4690-10-161

45. WHO (2013). Consolidated guidelines on the use of antiretroviral drugs for treating and preventing HIV infection. URL http://www.who.int/hiv/pub/guidelines/arv2013/download/en/index.html.

46. Wightman F, Ellenberg P, Churchill M, Lewin SR (2012) HDAC inhibitors in HIV. Immunol Cell Biol 90: 47–54. doi: 10.1038/icb.2011.95 PMID: 22083528

47. Ward H, Ronn M (2010) Contribution of sexually transmitted infections to the sexual transmission of HIV. Curr Opin HIV AIDS 5: 305–310. doi: 10.1097/COH.0b013e32833a8844 PMID: 20543605

48. Brenchley JM, Schacker TW, Ruff LE, Price DA, Taylor JH, et al. (2004) CD4+ T cell depletion during all stages of HIV disease occurs predominantly in the gastrointestinal tract. J Exp Med 200: 749–759. doi: 10.1084/jem.20040874 PMID: 15365096

49. Veazey RS, DeMaria M, Chalifoux LV, Shvetz DE, Pauley DR, et al. (1998) Gastrointestinal tract as a major site of CD4+ T cell depletion and viral replication in SIV infection. Science 280: 427–431. doi: 10.1126/science.280.5362.427 PMID: 9545219

50. Sáez-Ciríon A, Bacchus C, Hocqueloux L, Avettand-Fenoel V, Girault I, et al. (2013) Post-treatment HIV-1 controllers with a long-term virological remission after the interruption of early initiated antiretrovi-ral therapy anrs visconti study. PLoS Pathog 9: e1003211. doi: 10.1371/journal.ppat.1003211

51. Rizzardi GP, Harari A, Capiluppi B, Tambussi G, Ellefsen K, et al. (2002) Treatment of primary HIV-1 in-fection with cyclosporin A coupled with highly active antiretroviral therapy. J Clin Invest 109: 681–688. doi: 10.1172/JCI14522 PMID: 11877476

52. Lederman MM, Smeaton L, Smith KY, Rodriguez B, Pu M, et al. (2006) Cyclosporin A provides no sustained immunologic benefit to persons with chronic HIV-1 infection starting suppressive antiretroviral therapy: results of a randomized, controlled trial of the AIDS clinical trials group a5138. J Infect Dis 194: 1677–1685. doi: 10.1086/509261 PMID: 17109339

53. Lu W, Arraes LC, Ferreira WT, Andrieu JM (2004) Therapeutic dendritic-cell vaccine for chronic HIV-1 infection. Nat Med 10: 1359–1365. doi: 10.1038/nm1147 PMID: 15568033

54. Zhang C, Zhou S, Chain BM (2015). LeoTask: a fast, flexible and reliable framework for computational research. Preprint. Available: arXiv:1501.01678. Accessed 10 Feb 2015.